Model-based Needle Steering in Soft Tissue via Lateral Needle Actuation

Thomas Lehmann[1], Ronald Sloboda[2], Nawaid Usmani[3], and Mahdi Tavakoli[1]

***Abstract*—Needle insertion is a minimally invasive procedure finding applications in biopsy, ablation, drug delivery and cancer therapy. Prostate brachytherapy is a therapeutic procedure where radioactive agents are implanted within the prostate using long needles for the purpose of cancer irradiation. During insertion, each inserted needle needs to remain on a straight path due to dosage distribution requirements. This is difficult to achieve as the beveled needle tip causes needle deflection. A common method for the surgeon to steer beveled-tip needles manually is intermittent axial rotation. Over the last decade, substantial advancements have been made in robotic assistance during needle steering. The most common steering input has, however, been axial needle rotation. A novel needle steering input proposed and investigated recently by our research group is lateral needle actuation near the needle's entry point into tissue. The investigations have yielded promising results with respect to the overall steering potential and improving the steerability of the needle. In this work, a model-based control algorithm is presented that uses only lateral needle actuation to minimize needle deflection at the final insertion depth. The algorithm consists of two stages: an off-line trajectory planning stage and an on-line trajectory adjustment stage. Insertion experiments into phantom tissue were carried out to validate the proposed control algorithm. The results show that the algorithm is able to steer the needle towards the desired target while only using lateral needle actuation as steering input.**

***Index Terms*—Medical Robots and Systems; Surgical Robotics: Steerable Catheters/Needles; Force Control**

I. Introduction

NEEDLE insertion is a minimally invasive medical procedure in which needles are inserted into the body for the purpose of drug delivery, ablation, biopsy, or delivery of radioactive agents for cancer treatment. A popular procedure where rice-grain-sized radioactive seeds are implanted in the prostate for the purpose of cancer irradiation is prostate brachytherapy. Multiple low-dose-rate (LDR) seeds are implanted in and around the prostate gland. A total of approximately 16-20 hollow needles carrying rows of seeds are inserted successively by hand, guided by a 5 mm grid template (see Fig. 1). When the final insertion depth is reached, each needle is withdrawn while at the same time the seeds are pushed out using a stylet. This way, ideally multiple rows of seeds are implanted in parallel at distances defined by the grid template. The distribution of seeds is pre-planned to achieve the desired distribution of radiation across the cancer-affected prostate volume. During insertion and seed deposition, the location of the needle and deposited seeds is monitored by a trans-rectal ultrasound (TRUS) probe to facilitate accurate seed placement. For the radiation emitted by the seeds to be distributed efficiently throughout the prostate, it is important for the seeds to be deposited at their pre-planned locations. The target locations are registered with the template holes and, therefore, it is desirable that the needle remains on a straight trajectory during insertion. The seeds then apply a defined dosage of radiation to the cancerous tissue from close proximity, thus directly affecting the cancerous tissue while reducing radiation exposure to surrounding healthy tissue and organs. A critical assumption during pre-planning is that the needle remains on a straight trajectory during insertion. In clinical practice, however, this assumption does not hold well as the needle deflects from the desired straight trajectory due to its beveled tip. Thus, needle deflection can cause the seeds to be displaced from their desired locations within the prostate, which in turn causes an inefficient distribution of radiation and can therefore negatively affect treatment efficacy [1] [2].

The tip of brachytherapy needles is beveled to enable manual steering and to minimize cutting-induced tissue trauma. During insertion, the beveled tip causes the tissue to be displaced asymmetrically, which forces the needle to deflect in the same direction as the bevel. This feature of the beveled-tip needle can be used during insertion to steer the needle by simply intermittently rotating the needle axially to adjust the bevel direction and therefore the unadjusted direction of needle deflection as the needle is further inserted. This technique is in fact commonly applied during prostate brachytherapy. During insertion, the surgeon will insert the needle and observe the deflection through TRUS images. If an unacceptable amount of deflection is observed, the surgeon will manually rotate it by 180° about its insertion axis to steer the needle back towards the target. Rotation may be done intermittently throughout insertion rather than continuously to avoid tissue damage and out-of-plane deflection. The needle deflection needs to be

Manuscript received: February 23, 2018; Revised June 14, 2018; Accepted July 12, 2018.

This paper was recommended for publication by Editor Ken Masamune upon evaluation of the Associate Editor and Reviewers' comments. This work is supported by the Canada Foundation for Innovation (CFI) under grant LOF 28241, the Alberta Innovation and Advanced Education Ministry under Small Equipment Grant RCP-12-021, the Natural Sciences and Engineering Research Council (NSERC) of Canada under grant CHRP 446520, the Canadian Institutes of Health Research (CIHR) under grant CPG 127768, the Alberta Innovates - Health Solutions (AIHS) under grant CRIO 201201232 and by a University of Alberta startup grant.

[1]Thomas Lehmann (Corresponding Author) and Mahdi Tavakoli are with the Department of Electrical and Computer Engineering, University of Alberta, AB, Canada T6G 1H9. {lehmann, mahdi.tavakoli}@ualberta.ca

[2]Ronald Sloboda is with the Division of Medical Physics, Department of Oncology, Cross Cancer Institute, 11560 University Avenue, Edmonton, AB, Canada T6G 1Z2. ron.sloboda@albertahealthservices.ca.

[3]Nawaid Usmani is with the Department of Oncology, Cross Cancer Institute, 11560 University Avenue, Edmonton, AB, Canada, T6G 1Z2. nawaid.usmani@albertahealthservices.ca

Digital Object Identifier (DOI): see top of this page.

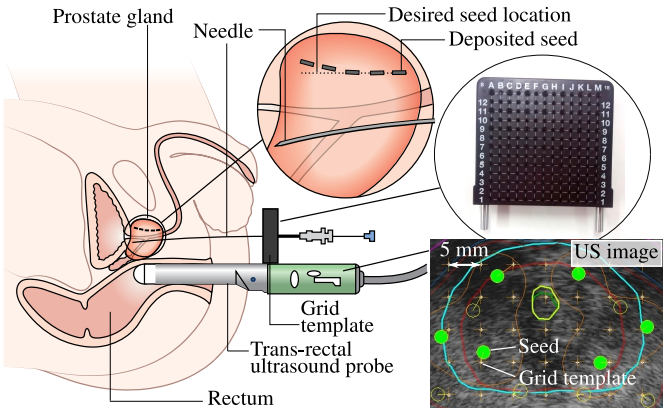

Fig. 1. A schematic representation of the radiation therapy procedure prostate brachytherapy. Radioactive seeds are implanted within the prostate with a needle guided by a grid template. The location of seed deposition is observed with a trans-rectal ultrasound (TRUS) probe (source: Cancer Research UK / Wikimedia Commons).

controlled by an experienced surgeon such that the needle shape at the final insertion depth reaches the target and is as close to the unbent needle as possible [3]. The absolute seed placement uncertainty is approximately ± 5 mm for manual placement by an expert practitioner [2].

A further method for steering the needle is the manual application of lateral force onto the needle shaft between the patient's skin and the grid template. The lateral force causes the shaft to be displaced laterally. When the force is applied at a shallow insertion depth and maintained during further insertion, the needle deflection can be significantly reduced [3], [4].

These methods of manual needle steering and trajectory control can be automated using robotic assistance to aid the surgeon during prostate brachytherapy and more generally during all needle insertion procedures. Extensive research has been conducted in various robotics-related fields such as needle-tissue interaction and needle deflection modeling, image-based deflection measurement, needle steering and deflection control, and robotic systems towards advancing automated needle steering techniques.

Substantial contributions have been made in needle-tissue interaction and deflection modeling [4]–[23]. The majority of the proposed modeling approaches are mechanics-based and take into account the tissue compression due to needle deflection and the bevel-induced force commonly referred to as *cutting force* that is modeled as a point load at the needle tip.

Other devised deflection models are kinematics-based [14], [19], [24]–[28], e.g. based on bicycle kinematics. Those models are, however, less directly associated with tissue properties but can nevertheless adequately model and predict multi-bend needle tip trajectories.

Various methods for needle steering that make use of the above-cited mechanics- and kinematics-based models [8], [11], [14], [21], [23]–[25], [27], [29]–[31] have also been proposed.

This paper proposes a novel needle steering method that uses lateral needle actuation near the needle entry point into tissue. Controlling the needle (tip) deflection towards the desired trajectory during insertion, e.g., zero tip deflection is commonly done through axial needle rotation in case of a bevel tip needle. A novel needle steering method using lateral needle actuation near the needle's entry point into tissue and a mathematical model based on the mechanics of the interactions between needle and tissue (mechanics-based) that can be used to predict the deflection of a needle exposed to lateral force and axial rotation was introduced by Lehmann *et al.* [4], [32]. The method for lateral actuation is schematically shown in Fig. 2. Naturally, the beveled tip of the needle is constrained to move on a circular trajectory during insertion meaning that needle steering using axial rotation only is an under-actuated control problem. This constraint to travel along the path cut by the needle tip can be significantly relaxed through lateral force as the needle tip can now be directly moved laterally thus increasing the needle tip's dexterity. An advantage of needle steering via lateral actuation is therefore that it allows for direct manipulation of needle deflection inside tissue and can be used to counter the deflection caused by the beveled needle tip and therefore bring the needle to a desired trajectory. These advantages have direct applications in prostate brachytherapy where the added dexterity can help to steer the needle towards the desired straight path.

It was shown previously that lateral actuation can contribute significantly to reducing the needle deflection in a way that is not possible with only a limited amount of intermittent axial needle rotations (e.g., one) to limit tissue trauma due to rotation-induced drilling effects [32]. Simulations using the developed deflection model also indicated that it is possible to steer the needle to a straight trajectory using only lateral actuation. This has, however, not been shown experimentally. As demonstrated in [4], at higher insertion depths, the influence of lateral force on the needle tip deflection declines. This is due to a combination of the needle being constrained by tissue and the needle's loss in resistance to bending with increasing needle length. The amount of force applied at a shallow insertion depth is therefore crucial for the amount of needle deflection at the depth section of interest. As also shown in [4], a primitive control law such as a simple PID controller is not sufficient to control deflection using lateral needle actuation. A deflection controller must be able to project the lateral force that needs to be applied at a shallow depth to reach the desired deflection at the final insertion depth. The behavior of the needle at a given insertion depth can be estimated and predicted with the deflection model presented in [4].

To further investigate the potential of lateral needle actuation for needle steering, in this paper, a model-based approach for needle steering using only lateral actuation is investigated. Only lateral actuation as steering input is considered as this explores the actuation method's potential beyond the simulations provided in [4].

The steering approach consists of two phases where during the first phase, the off-line trajectory planning phase, the desired needle tip trajectory is found that brings the needle to the desired target. During the second phase, as the needle is inserted, a real-time model-based algorithm for needle tip trajectory adjustment uses the US-image-based needle tip deflection measurement to adjust the applied lateral force such

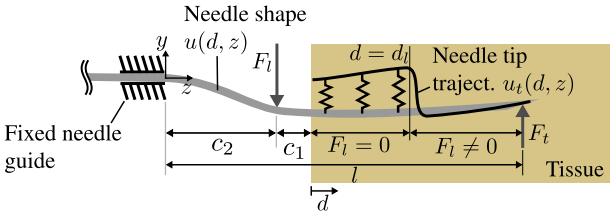

Fig. 2. A schematic representation of the inserted needle displaced by a point load F_l enacted by the lateral actuator. The tissue is modeled as virtual springs with the constant K.

that the error between the pre-planned needle tip trajectory and the measured needle tip deflection is minimized. In a scenario where the deflection model represents the needle deflection inside tissue entirely correctly, the second phase of real-time trajectory re-planning would not be needed. As, however, the deflection model introduced in [4] does, as most models representing physical systems, not perfectly represent the needle-tissue system, adjusting the lateral force online as needed is required to account for model inaccuracies.

II. Needle Steering Method

In any needle steering scenario, either the needle tip is steered towards a target point or a section of the needle must reach a desired line segment. Fig. 3 shows the latter needle steering objective where the needle's distance to the line segment τ at the final insertion depth must be minimized. In this study, the above steering objective is chosen as it is commonly found in prostate brachytherapy due to the reasons presented in Section I. As indicated by the simulation results presented in [4], this can be achieved through only the use of the control input lateral actuation.

A. Needle Deflection Modeling

In this section, a brief re-introduction of the deflection model proposed in [4] is given to provide a basis for the following derivations of a force model that is based on the deflection model. A schematic representation of the needle displaced by a lateral point load during insertion including the tissue reaction modeled as virtual springs is shown in Fig. 2. The needle-tissue interaction modeling is energy-based and considers the strain energy stored in the needle, the potential energy stored in the displaced tissue, the work done by the lateral force F_l and the tip force F_t (see Fig. 2). The needle-tissue interaction model formulation expressed as the system potential is then

$$\Pi(u) = \underbrace{\int_0^l \frac{EI}{2}\left(\frac{\partial^2 u(d,z)}{\partial z^2}\right)^2 dz}_{\text{Strain energy stored in the needle}} + \underbrace{\frac{K}{2}\int_{l-d}^{l}\Big(u(d,z)-u_t(d,z)\Big)^2 dz}_{\text{Energy stored in displaced tissue}} - \underbrace{F_l u(d,c_2)}_{\text{Work done by lateral force}} - \underbrace{F_t u(d,l)}_{\text{Work done by tip force}} \quad (1)$$

where $u(d,z)$ is the needle deflection shape and $u_t(d,z)$ is the needle tip trajectory. To solve (1) for the needle deflection shape $u(d,z)$, the Rayleigh-Ritz method is used where $u(d,z)$ is approximated with the finite series

$$u_n(d,z) = \sum_{i=1}^{n} q_i(z) g_i(d) \quad (2)$$

where $q_i(z)$ are sinusoidal approximation functions that must satisfy the system's boundary conditions. g_i are at this point unknown weighting coefficients. Inserting (2) into (1), and then taking the partial derivative of $\Pi(u_n)$ with respect to g_i, the linear system of equations

$$\underbrace{\begin{bmatrix}\phi_{11} & \cdots & \phi_{1n}\\ \vdots & \ddots & \vdots \\ \phi_{n1} & \cdots & \phi_{nn}\end{bmatrix}}_{\Phi}\mathbf{g}(d) = F_l\underbrace{\begin{bmatrix}q_1(c_2)\\ \vdots \\ q_n(c_2)\end{bmatrix}}_{\mathbf{q}(c_2)} + F_t\mathbf{1}_{n\times 1} + \underbrace{\begin{bmatrix}\omega_1\\ \vdots \\ \omega_n\end{bmatrix}}_{\Omega} \quad (3)$$

with

$$\phi_{ji}(z) = EI\int_0^l q_i''(z)q_j''(z)\,dz + K\int_{l-d}^{l} q_i(z)q_j(z)\,dz$$
$$\omega_j(z) = K\int_{l-d}^{l} u_t(d,z)q_j(z)\,dz$$

is obtained. This system is now solved for $\mathbf{g}(d)$, which is then inserted into (2) to obtain the approximation of the needle deflection shape u_n. A detailed derivation of the deflection model is provided in [4].

In the following sections, the needle steering method that uses the re-introduced model, and consists of an off-line trajectory planning and on-line trajectory adjustment phase, is proposed. Algorithm 1 and Algorithm 2 provide a general overview of the off-line and on-line phases, respectively.

B. Needle Tip Trajectory Planning

During the first phase of the needle steering approach that is carried out *before* needle insertion, the trajectory planner uses the needle deflection model re-introduced in Section II-A to find the optimal needle tip trajectory that steers the needle towards its target. The model is used to establish a cost function that minimizes the area A_e (see Fig. 3). Considering that generally, the search space for the lateral force profile is infinite, the simplified function

$$f_l(d,d_{l,1},d_{l,2}) = F_{l,c}\left[h(d-d_{l,1}) - h(d-d_{l,2})\right] \text{ for } d\in(0,d_f) \quad (4)$$

is chosen for the force profile to reduce the search space. The function $h(\cdot)$ is a step function, $F_{l,c}$, $d_{l,1}$, and $d_{l,2}$ represent the constant force magnitude, and the start and end depths at which the constant $F_{l,c}$ is applied, respectively. As shown in (4), the lateral force profile f_l is a function of d, $d_{l,1}$ and $d_{l,2}$. The cost function constructed from (4) that returns the residual between the target line section τ and the needle shape at the final insertion depth is given as

$$R(F_{l,c},d_{l,1}) = \sum_{z_\tau\in(d_s,d_f)}\Big(u(d_f,z_\tau,F_{l,c},d_{l,1}) - \tau\Big)^2 \quad (5)$$

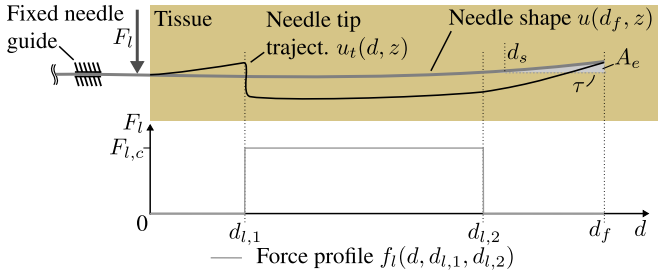

Fig. 3. The considered control objective commonly occurring during prostate brachytherapy, which is to minimize the area A_e under the line segment τ spanning from d_s to d_f. Shown also are the parameters $F_{l,c}$, $d_{l,1}$ and $d_{l,2}$ determined by needle tip trajectory planning in order to reach the objective of minimizing A_e.

and constitutes a sum of squared differences. $u(d_f, z_\tau, F_{l,c}, d_{l,1})$ is the simulated needle deflection at the final insertion depth obtained from the deflection model. The inputs to the cost function that are adjusted to minimize R are the constant lateral force magnitude $F_{l,c}$ and the application depth of $F_{l,c}$, $d_{l,1}$. The depth $d_{l,2}$ is chosen to be a depth where the lateral actuation ceases to be effective based on prior information apparent from experimental and simulation studies. The chosen optimization algorithm to find the optimal values of the parameters $F_{l,c}$ and $d_{l,1}$ and thus the optimal tip trajectory is pattern search [33]. The identified optimal tip trajectory is then used as reference trajectory for the on-line deflection control algorithm operating during insertion (see Algorithm 2).

Algorithm 1 The off-line trajectory planning algorithm.

K, F_t ▷ *Tissue stiffness and needle tip force, respectively (measured)*
$u_t^* \leftarrow$ PATTERNSEARCH(COSTFCN, $F_{l,c,\text{ini}}$, $d_{l,1,\text{ini}}$)
▷ *$F_{l,c}$ and $d_{l,1}$ are adjusted until residual R is at a minimum*
▷ *u_t^*: Optimal needle tip trajectory*
function COSTFCN($d_{l,1}$, $F_{l,c}$)
  $d \in (0, d_f)$ ▷ *d: Insertion depths*
  $f_l(d, d_{l,1}, d_{l,2}) = F_{l,c}\left[h(d-d_{l,1}) - h(d-d_{l,2})\right]$
  ▷ *Lateral force profile (see (4))*
  ▷ *$d_{l,2}$: Pre-defined constant depth*
  $u(d_f, z) \leftarrow$ CLC_NDL_TIP_TRJ(f_l, K, F_t) ▷ *Model proposed in [4]*
  ▷ *$u(d_f,z)$: Needle deflection (curvature) at d_f*
  $R = \sum_{z_\tau \in (d_s, d_f)} \left(u(d_f, z_\tau) - \tau\right)^2$ ▷ *See (5) & Fig. 3*
  ▷ *R: Residual (sum of squared difference between target τ and u)*
  return R
end function

Algorithm 2 The on-line trajectory adjustment algorithm.

$d \leftarrow d_0$ ▷ *d_0: Initial insertion depth*
$\delta \leftarrow$ PROCESS_US_IMAGE() ▷ *δ: Needle tip deflection at d*
$u_t(d,z) \leftarrow [u_t(d,z) \quad \delta]$
▷ *The current deflection is appended to the needle tip trajectory $u_t(d,z)$*
while $d < d_f$ **do**
  $\hat{d} \leftarrow d + \Delta d$ ▷ *$\hat{d}$: Prediction depth*
  $\hat{\delta} \leftarrow u_t^*(\hat{d})$ ▷ *u_t^*: Optimal needle tip trajectory (see Algorithm 1)*
  ▷ *$\hat{\delta}$: Optimal needle tip deflection at prediction depth $\hat{d}$*
  $\hat{F}_l \leftarrow$ CLC_LATERAL_FORCE($\hat{\delta}$, $u_t(d,z)$, K, F_t) ▷ *Implementation of (7)*
  ▷ *$\hat{F}_l$: Predicted lateral force at prediction depth $\hat{d}$*
  APPLY($\hat{F}_l$) ▷ *Apply the lateral force $\hat{F}_l$ to the needle*
  $\delta \leftarrow$ PROCESS_US_IMAGE()
  $u_t(d,z) \leftarrow [u_t(d,z) \quad \delta]$
end while

C. On-line Tip Trajectory Adjustment

During insertion, the lateral force applied onto the needle is adjusted based on the error between pre-planned needle tip trajectory and the measured needle tip deflection. Generally, it would be possible to use the force predicted during phase 1, the off-line trajectory planning phase, to steer the needle during insertion. Since, however, the deflection model's prediction accuracy cannot be fully guaranteed to be adequate due to modeling inaccuracies and possibly changing conditions in the physical system, the force needs to be re-calculated on-line based on deflection feedback that is measured via US imaging. To predict the lateral force that is required to bring the needle tip from its current position to the desired position, an inverse deflection model is needed that returns the lateral force based on the desired needle deflection. In the following, such a model is derived from the deflection model.

Let us consider a desired needle tip deflection $\hat{\delta} = \hat{u}(d + \Delta d, l)$ that we want to reach through applying a lateral force F_l that is yet to be determined. The variable Δd is the distance by which the needle is advanced. Let us also assume that the needle tip trajectory $u_t(d,z)$ up to the current depth d is known through measurement. In order to solve for the unknown lateral force F_l, (3) is first augmented with the vector $\Lambda = [\mathbf{0}_{n\times 1} \quad \hat{\delta}]^T$ followed by moving $F_l\mathbf{q}(c_2)$ to the right-hand side and merging $\mathbf{q}(c_2)$ into Φ. The new system of equations is then

$$\underbrace{\begin{bmatrix} \Phi & -\mathbf{q}(c_2) \\ \mathbf{1}_{1\times n} & 0 \end{bmatrix}}_{\Phi^\dagger} \underbrace{\begin{bmatrix} \mathbf{g} \\ F_l \end{bmatrix}}_{\mathbf{g}^\dagger} = \begin{bmatrix} F_t\mathbf{1}_{n\times 1} \\ 0 \end{bmatrix} + \underbrace{\begin{bmatrix} \Omega \\ 0 \end{bmatrix}}_{\Omega^\dagger} + \underbrace{\begin{bmatrix} \mathbf{0}_{n\times 1} \\ \hat{\delta} \end{bmatrix}}_{\Lambda}. \tag{6}$$

Finally, (6) is solved for $\mathbf{g}^\dagger$ as

$$\mathbf{g}^\dagger = \Phi^{\dagger -1}\left(F_t\mathbf{1}_{n\times 1} + \Omega^\dagger + \Lambda\right) \tag{7}$$

and the lateral force is $F_l = g^\dagger_{n+1}$.

With (7), we can now predict the necessary lateral force F_l for a desired tip deflection $\hat{\delta}$ given parameters K, F_t and the measured needle tip trajectory $u_t(d,z)$. When this model is implemented on a digital computer, the needle tip trajectory $u_t(d,z)$ is a vector of measured (or predicted) tip deflections as the needle is inserted. The advantage of this method of direct lateral force calculation (F_l) is that no time consuming iterative search is needed, which is crucial given sample time constraints during real-time trajectory re-planning.

During insertion, multiple criteria are enforced at which the lateral force is removed. This is to detect whether the influence of the lateral force on needle deflection has declined to a degree where the steering effect is no longer given, to prevent instability of the lateral actuator and to prevent application of excessive force. The criteria are that a maximal force limit $F_{l,\max}$ is exceeded, the limit for a change in lateral force between samples ΔF_l is exceeded and $d > d_{l,2}$. If any of these criteria is met, the lateral actuator's reference force is set to zero.

III. Experimental Study

A. Experimental Setup

The experimental system for manual needle insertion including a lateral needle actuation system is depicted in Fig. 4.

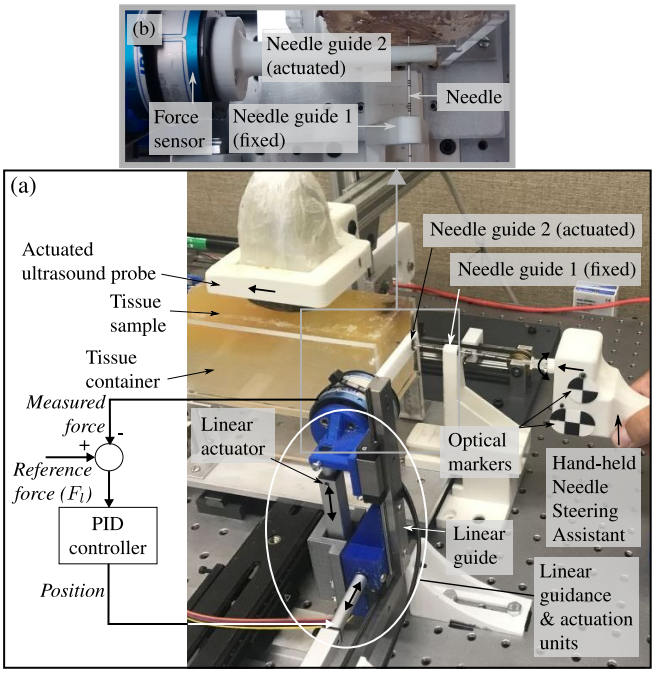

Fig. 4. The experimental robotic needle insertion system with (a) the total perspective of the setup and (b) a top-down close-up view of the needle being guided through the actuated and fixed needle guides.

It re-creates the setup used during prostate brachytherapy procedures with respect to needle observation methods and hardware such as the grid template. The system is designed to extend the current clinical hardware (see Fig. 1) while at the same time avoiding having to change the basic surgical setup or the procedure. It is designed to carry out steering actions automatically that would otherwise be carried out manually by the surgeon. The actions to manipulate the needle's trajectory, namely the application of lateral force and axial rotation, can be carried out automatically during insertion. In this work, the system's capability of axial needle rotation is, however, not used. The setup consists of a Hand-held Needle Steering Assistant (HNSA), which was developed by Rossa *et al.* [23] holding a standard 18G brachytherapy needle, a fixed needle guide (needle guide 1) and a second needle guide actuated by linear actuators (needle guide 2) and sensorized through a force/torque sensor that is mounted at the guide's base. Furthermore, an actuated ultrasound (US) probe is used to track the needle tip inside the phantom tissue sample during insertion. The HNSA [23] contains a miniature DC motor through which the needle can be rotated axially at the desired insertion depth. Affixed to the side of the HNSA are two optical markers used to continuously track its position during insertion with an optical tracker (MicronTracker, ClaroNav, Toronto, ON, Canada, not included in Fig. 4). Since the motion tracker is calibrated to the tissue container and the needle is assumed a rigid body in the insertion direction, the current needle insertion depth can be inferred from the measured HNSA location. Needle guide 1 is designed after a standard variant as used in prostate brachytherapy where its hole is made to fit the 18G brachytherapy needle precisely. Since needle guide 1 is mounted to the breadboard, the needle is restricted from moving laterally and pivoting within the guide.

During insertion, the needle is guided by needle guide 1 (fixed) and needle guide 2 (actuated). While guide 1 prevents the needle from pivoting, guide 2 is designed to allow the needle to pivot. Needle guide 2 can be displaced laterally to the axial needle direction through two perpendicularly mounted linear guidance and actuation units. Each linear guidance and actuation unit consists of a miniature linear guide (Type SSEBV16-150, MISUMI Group Inc., Tokyo, Japan) and a L16 Miniature Linear Actuator (Actuonix Motion Devices Inc., Victoria, BC, Canada). The units are mounted in serial and confine needle guide 2's motions to a plane normal to the axial needle direction. The forces exerted by the guide onto the needle are measured by a 6 degree-of-freedom (DOF) force/torque (f/t) sensor (50M31A3-I25, JR3 Inc., Woodland, CA, USA). The f/t sensor is used to control the lateral force applied by the actuated guide through a PID force controller. Due to the small hole depth (1.7 mm) of the actuated needle guide, the needle can pivot within the guide and friction between guide and needle is negligible.

To track the needle cross-section for needle deflection measurement in real-time during insertion, a modified version of the algorithm introduced by Carriere *et al.* [34] is used.

B. Results

An experimental insertion study is carried out to assess the steering accuracy of the proposed needle steering method. The distance between fixed needle guide and the tissue is set to 36 mm. A standard brachytherapy needle (Type RP-1100-1820, Riverpoint Medical, Portland, OR, USA) is inserted into two samples of phantom tissue made from Plastisol (Type Super Soft Plastic, M-F Manufacturing Co., Inc, Fort Worth, TX, USA) with different stiffness. The tissue Young's modulus K and needle tip force F_t need to be identified to parameterize the deflection and force models. To measure the tissue Young's modulus, the same indentation method as described in [4] is used. The identified Young's modulus K of tissue 1 is 12.16±2.5 kPa and of tissue 2 it is 14.18±4.25 kPa.

Six insertions are carried out into each tissue sample to a final depth of 140 mm without applying lateral force to identify the tip force F_t, which is then quantified using the method described in [4] for each tissue sample. The identified tip force for tissue 1 is 0.25 N and for tissue 2 it is 0.29 N. With the deflection model now parameterized for each tissue sample, the optimal needle trajectory can be determined using the method described in Section II-B. The identified parameter values of the constant lateral force $F_{l,c}$ and the force's application depth $d_{l,1}$ with which the optimal trajectory is achieved are -2.98 N and 10.5 mm, respectively, for tissue 1, and -3.43 N and 10.5 mm for tissue 2.

During the insertions, the needle is steered in real-time through the application of lateral actuation only and using the algorithm introduced in Section II-C. Six insertions are carried out into each Plastisol tissue sample while a lateral force is applied that steers the needle to the pre-planned target. The experimental results are plotted in Fig. 5. The measured needle tip trajectories of the six insertions where lateral actuation

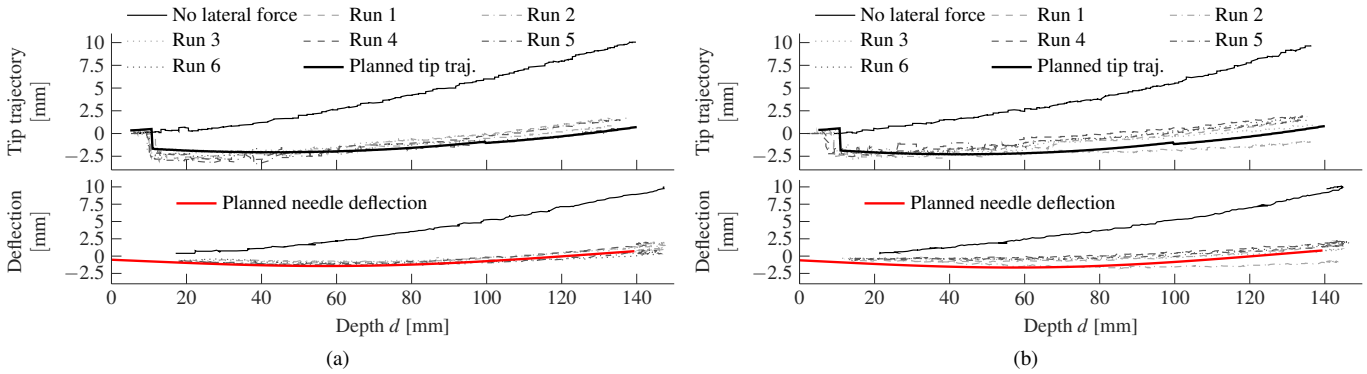

Fig. 5. Results of needle insertion experiments. The needle is steered by the proposed lateral force method for the tissue stiffnesses (a) 12.16 kPa and (b) 14.18 kPa. Each of the figures (a) and (b) shows the planned and measured needle tip trajectories (top plot) and the measured needle deflection shape at the final insertion depth of 140 mm (bottom plot) for all six insertion trials. The needle tip trajectories are measured during insertion as the ultrasound probe tracks the tip. The needle deflection shape in is measured after the final insertion depth has been reached and insertion is stopped.

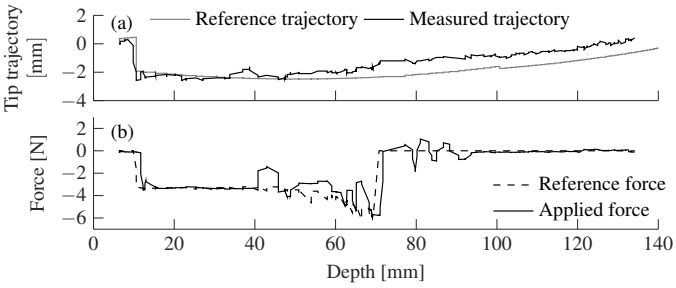

Fig. 6. (a) The reference and measured needle tip trajectory during Run 6 and (b) the model-predicted and applied lateral force during insertion into tissue sample 1.

is used are plotted in the top plots of Fig. 5a and Fig. 5b for tissue 1 and tissue 2, respectively. To assess the steering accuracy and amount of deflection reduction, the pre-planned tip trajectory and a tip trajectory without lateral actuation are plotted. The maximum error between the measured and pre-planned needle tip deflection is approximately 2 mm at the final insertion depth. A substantial reduction of needle deflection of approximately 80% can be observed when the needle is steered using lateral actuation. To provide an assessment of the amount of residual needle deflection at the final insertion depth, the measured needle deflection at the final insertion depth for all 6 steered insertions and one non-steered insertion is plotted in the bottom plots of Fig. 5a and Fig. 5b for tissue 1 and tissue 2, respectively. The plots show that the deflection remains below approximately 2 mm throughout the entire needle length.

In Fig. 6a, the pre-planned and measured tip trajectory of Run 6 are plotted and in Fig. 6b, the corresponding reference and applied lateral force are plotted. In Fig. 6b it can be observed that the lateral force is removed at a depth of roughly 70 mm. The reference force is set to zero when one of the above mentioned criteria is met, which are in this case $F_{l,\max} = 8$ N, $\Delta F_l = 4$ N and $d_l = 100$ mm.

IV. Discussion

A significant reduction of needle deflection can be achieved while only using lateral actuation as steering input as described in Section III. This fact confirms the findings presented in [4] where simulations indicate that a lateral force applied continuously from a shallow insertion depth onward can substantially reduce needle deflection. The control method validated in this work also shows vastly superior performance compared to the simulated PID-based and ad-hoc control strategy employed in [4]. The experimental results also show that a needle deflection of approximately 2 mm remains (see Fig. 5b) that cannot be accounted for by the on-line algorithm for needle adjustment. This error could be further corrected by adjusting the model parameters tissue Young's modulus K and tip force F_t in an intelligent manner based on the error between predicted and measured deflection or by adding axial needle rotation as a steering input as needed.

Furthermore, Fig. 6b shows that the absolute maximum lateral force magnitude predicted on-line by the model and thus applied during the experiments is with 6 N much higher than the pre-planned absolute constant force of 2.98 N. In a clinical scenario, forces of such magnitude could exceed a limit that would prevent trauma to the patient. Given this limitation potentially imposed on lateral actuation, the steering objective might not be reachable entirely. This limitation suggests that lateral actuation alone as control input is in certain cases not enough to minimize needle deflection and a combination of lateral actuation and axial rotation should be used as needed.

V. Conclusion & Future Work

This paper proposes a method for needle steering using only lateral needle actuation as steering input. It was shown experimentally that the steering method can achieve a good performance for a steering objective that is pertinent to the efficient seed placement during prostate brachytherapy. It is also experimentally shown that it is possible to nearly eliminate needle deflection at the final insertion depth when applying only lateral needle actuation as the steering input. However, limitations with respect to the reachability of a target

potentially exist in case the lateral force needs to be limited during a clinical scenario to avoid inflicting trauma to the patient. Thus, a combination of intermittent axial rotation and lateral actuation can be considered to reach a desired steering objective despite a strict lateral force limit.

The limitations of the proposed steering method mentioned in Section IV need to be addressed in the future work. Further development of the model-based deflection controller should enable it to decide automatically on appropriate control actions lateral actuation and axial rotation under constraints and limiting conditions such as a limit on the lateral force or a limited amount of axial rotations. An automatic needle deflection controller should be able to autonomously choose and leverage the required control action based on the needle steering target.

REFERENCES

[1] P. L. Roberson, V. Narayana, D. L. McShan, R. J. Winfield, and P. W. McLaughlin, "Source placement error for permanent implant of the prostate," *Medical Physics*, vol. 24, no. 2, pp. 251–257, 1997.

[2] R. Taschereau, J. Pouliot, J. Roy, and D. Tremblay, "Seed misplacement and stabilizing needles in transperineal permanent prostate implants," *Radiotherapy and Oncology*, vol. 55, no. 1, pp. 59–63, 2000.

[3] M. Jamaluddin, S. Ghosh, M. Waine, M. Tavakoli, J. Amanie, A. Murtha, D. Yee, and N. Usmani, "Intraoperative factors associated with stranded source placement accuracy in low-dose-rate prostate brachytherapy," *Brachytherapy*, vol. 16, no. 3, pp. 497–502, 2017.

[4] T. Lehmann, C. Rossa, N. Usmani, R. Sloboda, and M. Tavakoli, "Deflection modeling for a needle actuated by lateral force and axial rotation during insertion in soft phantom tissue," *Mechatronics*, vol. 48, pp. 42 – 53, 2017.

[5] H. Kataoka, T. Washio, M. Audette, and K. Mizuhara, "A model for relations between needle deflection, force, and thickness on needle penetration," in *Medical Image Computing and Computer-Assisted Intervention - MICCAI 2001*, ser. Lecture Notes in Computer Science. Berlin, Heidelberg: Springer, 2001, vol. 2208, ch. 115, pp. 966–974.

[6] A. Okamura, C. Simone, and M. O'Leary, "Force modeling for needle insertion into soft tissue," *IEEE Transactions on Biomedical Engineering*, vol. 51, no. 10, pp. 1707–1716, 2004.

[7] T. Podder, J. Sherman, E. Messing, D. Rubens, D. Fuller, J. Strang, R. Brasacchio, and Y. Yu, "Needle insertion force estimation model using procedure-specific and patient-specific criteria," in *Proceedings of the 2006 International Conference of the IEEE Engineering in Medicine and Biology Society*, 2006, pp. 555–558.

[8] N. Abolhassani, R. Patel, and F. Ayazi, "Minimization of needle deflection in robot-assisted percutaneous therapy," *The International Journal of Medical Robotics and Computer Assisted Surgery*, vol. 3, no. 2, pp. 140–148, 2007.

[9] E. Dehghan, X. Wen, R. Zahiri-Azar, M. Marchal, and S. E. Salcudean, "Needle-tissue interaction modeling using ultrasound-based motion estimation : Phantom study," *Computer Aided Surgery*, vol. 13, no. 5, pp. 265–280, 2008.

[10] S. Misra, K. B. Reed, A. S. Douglas, K. T. Ramesh, and A. M. Okamura, "Needle-tissue interaction forces for bevel-tip steerable needles," in *Proceedings of the 2008 IEEE International Conference on Biomedical Robotics and Biomechatronics*, 2008, pp. 224–231.

[11] S. Misra, K. B. Reed, B. W. Schafer, K. T. Ramesh, and A. M. Okamura, "Mechanics of flexible needles robotically steered through soft tissue," *The International Journal of Robotics Research*, vol. 29, no. 13, pp. 1640–1660, 2010.

[12] R. Roesthuis, Y. V. Veen, A. Jahya, and S. Misra, "Mechanics of needle-tissue interaction," in *Proceedings of the 2011 IEEE International Conference on Intelligent Robots and Systems*, 2011, pp. 2557–2563.

[13] A. Asadian, M. R. Kermani, and R. V. Patel, "A novel force modeling scheme for needle insertion using multiple kalman filters," *IEEE Transactions on Instrumentation and Measurement*, vol. 61, no. 2, pp. 429–438, 2012.

[14] M. Abayazid, R. Roesthuis, R. Reilink, and S. Misra, "Integrating deflection models and image feedback for real-time flexible needle steering," *IEEE Transactions on Robotics*, vol. 29, no. 2, pp. 542–553, 2013.

[15] A. L. G. Robert, G. Chagnon, I. Bricault, P. Cinquin, and A. Moreau-Gaudry, "A generic three-dimensional static force distribution basis for a medical needle inserted into soft tissue," *Journal of the Mechanical Behavior of Biomedical Materials*, vol. 28, pp. 156–170, 2013.

[16] T. Lehmann, M. Tavakoli, N. Usmani, and R. Sloboda, "Force-sensor-based estimation of needle tip deflection in brachytherapy," *Journal of Sensors*, vol. 2013, pp. 1–10, 2013.

[17] C. Rossa, R. Sloboda, N. Usmani, and M. Tavakoli, "Estimating needle tip deflection in biological tissue from a single transverse ultrasound image: application to brachytherapy," *International Journal of Computer Assisted Radiology and Surgery*, vol. 11, no. 7, pp. 1347–1359, 2016.

[18] M. Khadem, B. Fallahi, C. Rossa, R. S. Sloboda, N. Usmani, and M. Tavakoli, "A mechanics-based model for simulation and control of flexible needle insertion in soft tissue," in *Proceedings of the 2015 IEEE International Conference on Robotics and Automation*, 2015, pp. 2264–2269.

[19] M. Khadem, C. Rossa, N. Usmani, R. S. Sloboda, and M. Tavakoli, "A two-body rigid/flexible model of needle steering dynamics in soft tissue," *IEEE/ASME Transactions on Mechatronics*, vol. 21, no. 5, pp. 2352–2364, 2016.

[20] T. Lehmann, C. Rossa, N. Usmani, R. S. Sloboda, and M. Tavakoli, "A real-time estimator for needle deflection during insertion into soft tissue based on adaptive modeling of needle-tissue interactions," *IEEE/ASME Transactions on Mechatronics*, vol. 21, no. 6, pp. 2601–2612, 2016.

[21] C. Rossa, M. Khadem, R. Sloboda, N. Usmani, and M. Tavakoli, "Adaptive quasi-static modelling of needle deflection during steering in soft tissue," *IEEE Robotics and Automation Letters*, vol. 1, no. 2, pp. 916–923, 2016.

[22] H. Lee and J. Kim, "Estimation of needle deflection in layered soft tissue for robotic needle steering," in *Intelligent Autonomous Systems 13: Proceedings of the 13th International Conference IAS-13*. Springer International Publishing, 2016, pp. 1133–1144.

[23] C. Rossa, N. Usmani, R. Sloboda, and M. Tavakoli, "A hand-held assistant for semiautomated percutaneous needle steering," *IEEE Transactions on Biomedical Engineering*, vol. 64, no. 3, pp. 637–648, 2017.

[24] R. J. Webster, J. S. Kim, N. J. Cowan, G. S. Chirikjian, and A. M. Okamura, "Nonholonomic modeling of needle steering," *The International Journal of Robotics Research*, vol. 25, no. 5-6, pp. 509–525, 2006.

[25] D. Glozman and M. Shoham, "Image-guided robotic flexible needle steering," *IEEE Transactions on Robotics*, vol. 23, no. 3, pp. 459–467, 2007.

[26] S. Misra, K. B. Reed, B. W. Schafer, K. T. Ramesh, and A. M. Okamura, "Observations and models for needle-tissue interactions," in *Proceedings of the 2009 IEEE International Conference on Robotics and Automation*, 2009, pp. 2687–2692.

[27] S. Patil, J. Burgner, R. J. Webster, and R. Alterovitz, "Needle steering in 3-D via rapid replanning," *IEEE Transactions on Robotics*, vol. 30, no. 4, pp. 853–864, 2014.

[28] B. Fallahi, M. Khadem, C. Rossa, R. Sloboda, N. Usmani, and M. Tavakoli, "Extended bicycle model for needle steering in soft tissue," in *Proceedings of the 2015 IEEE International Conference on Intelligent Robots and Systems*, 2015, pp. 4375–4380.

[29] P. Moreira and S. Misra, "Biomechanics-based curvature estimation for ultrasound-guided flexible needle steering in biological tissues," *Annals of Biomedical Engineering*, vol. 43, no. 8, pp. 1716–1726, 2014.

[30] J. Wang, X. Li, J. Zheng, and D. Sun, "Dynamic path planning for inserting a steerable needle into a soft tissue," *IEEE/ASME Transactions on Mechatronics*, vol. 19, no. 2, pp. 549–558, 2014.

[31] M. Khadem, C. Rossa, R. S. Sloboda, N. Usmani, and M. Tavakoli, "Ultrasound-Guided Model Predictive Control of Needle Steering in Biological Tissue," *Journal of Medical Robotics Research*, vol. 01, no. 01, p. 1640007, 2016.

[32] T. Lehmann, R. Sloboda, N. Usmani, and M. Tavakoli, "Human-machine collaboration modalities for semi-automated needle insertion into soft tissue," *IEEE Robotics and Automation Letters*, vol. 3, no. 1, pp. 477–483, 2018.

[33] R. Hooke and T. A. Jeeves, ""direct search" solution of numerical and statistical problems," *Journal of the ACM*, vol. 8, no. 2, pp. 212–229, 1961.

[34] J. Carriere, C. Rossa, R. Sloboda, N. Usmani, and M. Tavakoli, "Real-time needle shape prediction in soft-tissue based on image segmentation and particle filtering," in *Proceedings of the 2016 IEEE International Conference on Advanced Intelligent Mechatronics*, 2016, pp. 1204–1209.